

PROCEEDINGS OF SPIE

SPIDigitalLibrary.org/conference-proceedings-of-spie

A coded excitation framework for increased signal-to-noise ratio of in vivo ultrasound power Doppler imaging

Vienneau, Emelina, Byram, Brett

Emelina P. Vienneau, Brett C. Byram, "A coded excitation framework for increased signal-to-noise ratio of in vivo ultrasound power Doppler imaging," Proc. SPIE 11602, Medical Imaging 2021: Ultrasonic Imaging and Tomography, 116020P (15 February 2021); doi: 10.1117/12.2582344

SPIE.

Event: SPIE Medical Imaging, 2021, Online Only

A Coded Excitation Framework for Increased Signal-to-Noise Ratio of *in Vivo* Ultrasound Power Doppler Imaging

Emelina P. Vienneau^{*a}, Brett C. Byram^a

^aDepartment of Biomedical Engineering, Vanderbilt University, Nashville, TN, USA

ABSTRACT

Ultrasound power Doppler imaging is a useful clinical tool for measuring perfusion. Sensitivity to slow moving blood flow is important for many clinical applications, but thick abdominal walls or the presence of bone such as ribs or the skull cause significant attenuation and thereby reduce the signal-to-noise ratio (SNR) and flow sensitivity. One way to improve SNR is to inject microbubble contrast agents into the vascular system, but this is impractical for many applications. An alternative approach is to use coded excitation, a signal processing technique that can drastically increase SNR within FDA safety limits without contrast agents. This work encompasses a method to design long coded pulses that are simple to implement along with a pulse compression technique to completely suppress range lobes, thereby recovering axial resolution, maintaining contrast, and improving SNR by as much as a factor of $10\log_{10}(\text{code length})$. In simulations we show that this approach reliably improves the SNR of power Doppler imaging across a range of noise levels. As the noise level increases with respect to the blood, contrast and contrast-to-noise ratio are maintained with coded excitation whereas they drop precipitously without coded excitation. *In vivo* feasibility is also shown in transcranial and transthoracic cardiac B-Mode imaging. Both simulation and *in vivo* results match theoretical expectations of SNR gain. Finally, preliminary results showing *in vivo* power Doppler imaging in the liver are presented as well. Coded excitation is able to improve the blood vessel to background CNR and CR as compared to a standard approach.

Keywords: coded excitation, signal processing, power Doppler imaging, blood flow imaging, signal-to-noise ratio, image quality, inverse filtering, compound Barker codes

1. INTRODUCTION

Sensitivity to slow blood flow is important for applications such as assessment of cancer treatment with embolic agents (eg, TACE) and measuring functional hyperemia due to muscle contraction or neural activation. However, thick abdominal walls or the presence of bone such as ribs or the skull cause significant attenuation and thereby reduce the signal-to-noise ratio (SNR). This in turn reduces sensitivity to slow moving blood flow and increases the minimum detectable velocity. One way to improve SNR is to inject microbubble contrast agents into the vascular system, but this increases the scan time, complexity, and invasiveness of the procedure, ultimately rendering it impractical for many applications. An alternative approach is to use coded excitation, a signal processing technique that can dramatically increase SNR within FDA safety limits without contrast agents. Coded excitation works by increasing the time-bandwidth product of the transmitted pulse via frequency and/or phase modulation so that the pulse is lengthened and the total energy delivered is increased. The received data then undergoes pulse compression to recover the original axial resolution as defined by the base pulse, resulting in a high-SNR, high-resolution signal. Pulse compression is usually performed by a matched filter, but there are also mismatched filtering approaches that have been designed to further suppress range lobes. Design of a coded excitation framework in medical ultrasound must take several factors into consideration, including the SNR gain, the range lobe levels, the complexity of implementation, and robustness to motion and frequency-dependent attenuation [1]. The approach described herein optimizes for these design considerations. Long, compound Barker codes are used instead of standard Barker codes to provide larger SNR gains, inverse filtering is used instead of matched or mismatched filtering for greater range lobe suppression, single-transmit phase encoding is used instead of multiple-transmit phase encoding (ie, Golay codes) for reduced sensitivity to motion, and phase modulation is used instead of frequency modulation (ie, chirps) for simplicity and ease of implementation. In particular, this framework can be easily implemented on most ultrasound scanners such as the Verasonics that only have tri-state pulsers as opposed to multi-state pulsers. Although the use of compound Barker codes and inverse filtering have both been reported separately in the literature [2]–[6], this work is the first to the authors' knowledge to combine these two techniques for coded excitation in medical ultrasound. The goal of this work is to demonstrate the feasibility and efficacy of this coded excitation framework for increasing the SNR of power Doppler imaging, which is of particular importance in challenging *in vivo* scenarios.

2. METHODS

2.1 Principles of Coded Excitation Framework

To create the phase encoded excitation waveform, a long binary code is first created by computing the Kronecker product of two Barker codes. For example, the Kronecker product of two 3 bit Barker codes (1 1 -1) would be (1 1 -1 1 1 -1 -1 -1 1). This compound code is then up-sampled and convolved with a chip pulse to create a phase encoded excitation waveform. The chip is a base pulse that fits within the bandwidth of the transducer and defines the axial resolution. In this case it is a single cycle sinusoid. In order to have near-perfect range lobe suppression, an inverse filtering approach should be used instead of a traditional matched filter [2]–[4]. Barker codes longer than 2 bits as well as the Kronecker product of such Barker codes have this property. For example, the discrete Fourier transform of a 5x5 (25 bit) compound Barker code is shown in Figure 1a (note the code was zero-padded before computing the DFT). Since this binary code has full spectral support, a stable L-tap FIR filter can be designed to approximate the inverse spectrum. The inverse spectrum is also up-sampled and convolved with the chip waveform to create the final decoding filter which serves as an inverse for the phase encoding and a matched filter for the chip waveform. In Figure 1b, a 64 tap filter is shown for a 5x5 compound Barker code and a 2.7 MHz single cycle sine wave chip. The longer the binary code, the more taps are needed. By convolving this decoding filter with the received data in the time domain, pulse compression is achieved as shown in Figure 1c. For comparison, Figure 1c also shows the matched filter results and results of a standard, uncoded approach in which only the chip waveform was transmitted. In the left panel of Figure 1c, it is clear that the matched filter and the inverse filter achieve an amplitude gain of 25 with respect to the uncoded approach, corresponding to the time-bandwidth product of the coded excitation. From the right panel of Figure 1c, it is clear that the matched filtering approach produces very high undesirable range lobes at about -10 dB. The axial resolution of all three approaches is equivalent, demonstrating perfect pulse compression in this idealized scenario. Note that in the right panel of Figure 1c, the pulses were shifted such that their maxima were all at 0 dB.

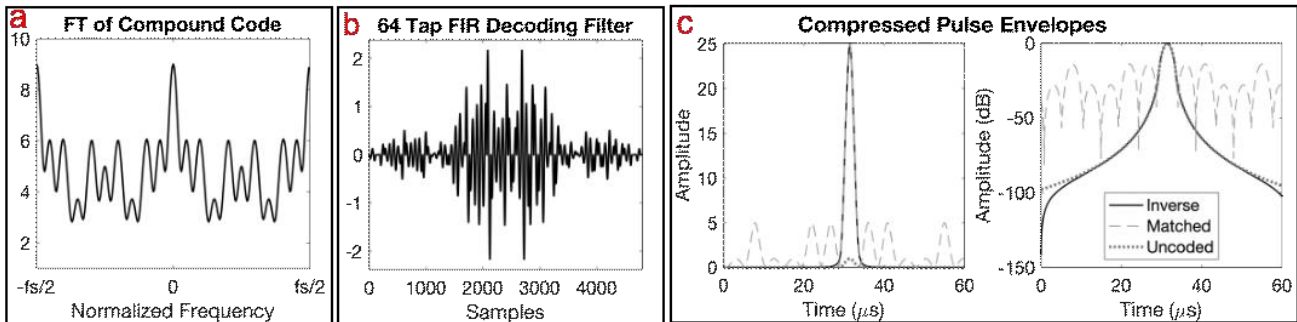


Figure 1: Principles of pulse compression in an ideal scenario. **a.** The Fourier transform of the 5x5 compound Barker code. **b.** 64 tap FIR pseudo-inverse filter for a 5x5 compound Barker Code and a 2.7 MHz single cycle sine chip. **c.** Pulse compression with the proposed inverse filter and with the standard matched filter. Uncoded approach shown for comparison.

2.2 Field II Blood Flow Simulations

To simulate blood flow imaging with coded excitation, Field II simulations were performed using Matlab [7], [8]. A 20 x 10 x 35 mm scattering phantom with 16 scatterers per resolution cell was created with a 2 mm diameter blood vessel angled at 45° from the transducer surface. The blood flow was parabolic with a peak velocity of 6 cm/s. The blood-to-tissue level was -60 dB. Gaussian noise was also added at noise-to-blood levels of -20, -10, 0, 10, and 20 dB with respect to the uncoded image. Imaging with a 128-element array (pitch = $\lambda/2$) was simulated for a 7 MHz imaging frequency and a $20f_0$ MHz sampling frequency. A plane wave synthetic aperture sequence was used with angles from -8° to 8° spaced by 2°. The final frame rate was 1 kHz and the total scan time was 0.1 s, corresponding to 100 slow-time acquisitions. The excitation waveforms used were a single cycle sine wave (baseline uncoded approach) and a 5x5 compound Barker code. A 128-tap FIR pseudo-inverse filter was used for decoding. Decoding was performed before beamforming. Clutter filtering was performed after beamforming with a 6th order Chebyshev IIR filter with a cutoff of 2 Hz.

2.3 Phantom and *in vivo* B-Mode Data Acquisition

To demonstrate feasibility of applying this coded excitation scheme to physically acquired data, a CIRS phantom was scanned with and without coded excitation. The excitation waveforms used were a single cycle sine wave (uncoded

approach), a 5 bit Barker code, a 13 bit Barker code, and a 5x5 (length 25) compound Barker code. All excitation waveforms had matched ISPPA₃ and the acoustic output of all sequences was measured with a hydrophone to ensure compliance with FDA safety guidelines. A 128-tap FIR filter was used when decoding. A 64-element P4-2v phased array (300 μm pitch) operating at 2.7 MHz and a Verasonics Vantage 128 system were used for imaging. The transmit focus was 8 cm and dynamic receive beamforming was applied. Ten frames were acquired in order to estimate SNR via normalized cross-correlation.

To further showcase the robustness of this framework to high noise *in vivo* imaging environments, transcranial B-Mode imaging was performed on five healthy adult subjects using the same sequences and parameters as specified above. Transthoracic cardiac B-Mode imaging was also performed on one healthy adult subject with an imaging frequency of 4.7 MHz. However, due to a low PRF and unmitigated out-of-plane subject/sonographer motion in these *in vivo* images, normalized-cross correlation estimates were far lower than expected and did not match qualitative assessments of SNR gain. In order to estimate the SNR gain for these *in vivo* cases, the amplitudes within bright ROIs in the skull and myocardial wall were also compared.

2.4 *In vivo* Power Doppler Data Acquisition

In vivo blood flow data was also acquired in the liver of a healthy adult subject. The excitation waveforms used were a single cycle sine wave (uncoded approach) and a 5x5 (length 25) compound Barker code. A 128-tap FIR filter was used for decoding. A 50 mm L12-5 linear array (195.3 μm pitch) operating at 5.2 MHz and a Verasonics Vantage 128 system were used for imaging. Only the first 128 of the 256 elements were used for transmit and receive. The imaging depth was 4 cm. A focused B-Mode image (2 cm transmit focus) was acquired for targeting purposes as well as a time series of plane wave synthetic aperture (PWSA) frames to measure blood flow. The PWSA sequence consisted of 320 frames of 16 angles from -7° to 8° degrees with a final PRF of 1 kHz, corresponding to a total scan time of 320 ms for the PWSA sequence. Clutter and noise filtering were performed with a singular value decomposition similar to the approach in [9]. Coded and uncoded images were acquired in quick succession, but due to subject breathing and sonographer hand motion, the FOVs between each image were not perfectly matched.

2.5 Image Quality Assessment

In order to quantify the image quality improvements from coded excitation, the blood vessel to background contrast-to-noise ratio (CNR) and contrast ratio (CR) were computed according to Equations 1 and 2, respectively. Note that these metrics were computed after clutter filtering. SNR was calculated on the enveloped data before clutter filtering according to Equation 3. For the *in vivo* and physical phantom images, ρ was estimated via normalized cross-correlation (NCC).

$$\text{CNR} = \frac{|S_t - S_o|}{\sqrt{\sigma_t^2 + \sigma_o^2}} \quad (1)$$

$$\text{CR} = 10 \log_{10} \left(\frac{\mu_t}{\mu_o} \right) \quad (2)$$

$$\text{SNR} = 10 \log_{10} \left(\frac{\rho}{1-\rho} \right) \quad (3)$$

3. RESULTS AND DISCUSSION

3.1 Field II Blood Flow Simulation Results

The results of the Field II blood flow simulations are shown in Figure 2. Qualitatively, the coded excitation images show much higher and more consistent contrast and CNR across noise levels, showing the advantage of using coded excitation in high noise environments. The individual CNR and CR metrics are provided in each of the power Doppler images (Figure 2 b-k). Excluding the matched filter gain from the chip portion of the decoding filter, the SNR gains for the 20, 10, 0, -10, and -20 dB blood-to-noise images were 12.89, 12.91, 12.93, 12.91, 12.91, respectively, indicating that this technique is able to produce a reliable SNR gain across varying noise levels. The theoretical SNR gain should be $10 \log_{10}(25) = 13.98$ dB. The remaining ~1 dB of unrealized gain could be due to inefficiencies in inverse filtering or slight imperfections in code compression, but these results still agree well with theoretical expectations.

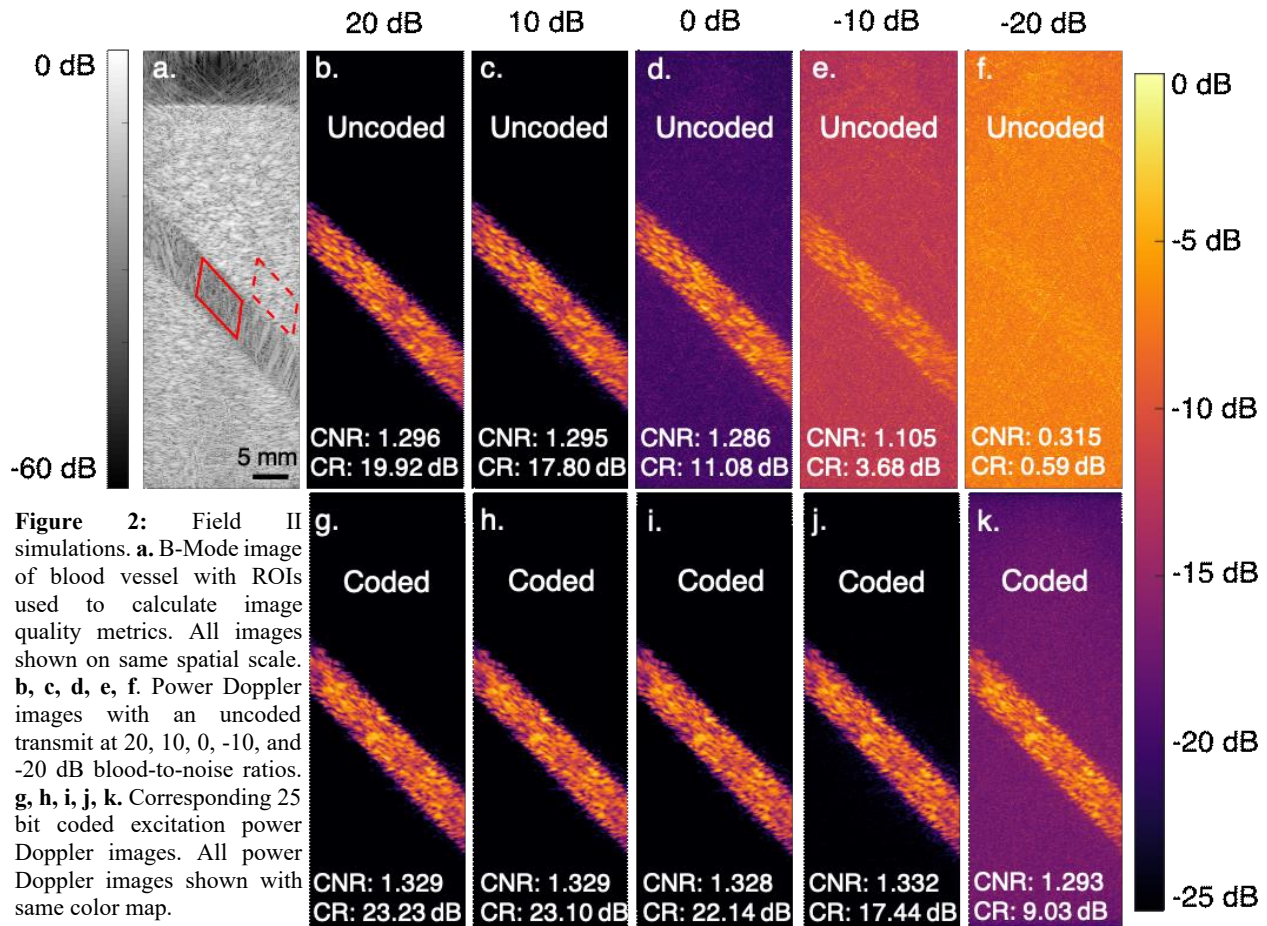


Figure 2: Field II simulations. **a.** B-Mode image of blood vessel with ROIs used to calculate image quality metrics. All images shown on same spatial scale. **b, c, d, e, f.** Power Doppler images with an uncoded transmit at 20, 10, 0, -10, and -20 dB blood-to-noise ratios. **g, h, i, j, k.** Corresponding 25 bit coded excitation power Doppler images. All power Doppler images shown with same color map.

Figure 3 shows the CNR, CR, and SNR of coded versus uncoded approaches across the same range of blood-to-noise levels. The SNR gain is constant across noise levels. However, the contrast and CNR gains are greater the higher the noise levels are with respect to the blood. These results highlight the benefit of using coded excitation in high noise environments such as in difficult-to-image patients and in particularly challenging scenarios such as imaging through the bone.

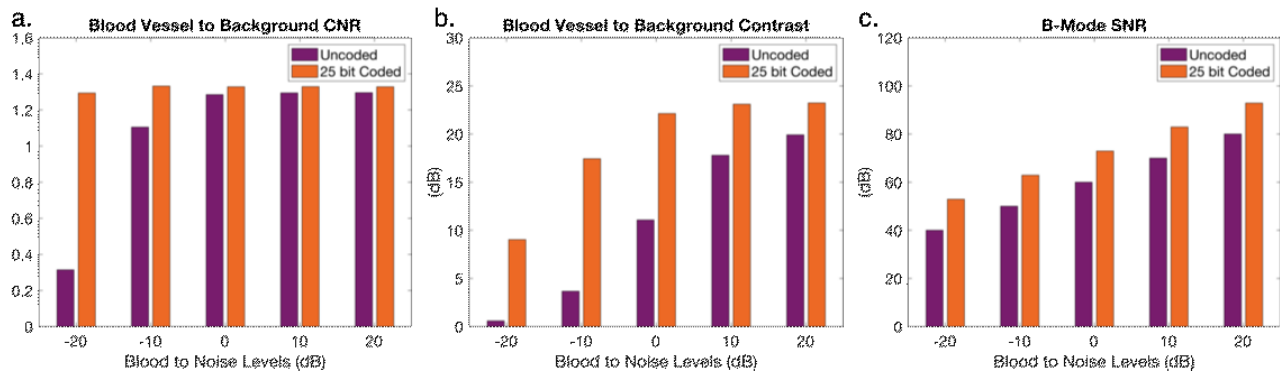


Figure 3: Bar graphs comparing image quality metrics between coded and uncoded excitation approaches. **a.** Contrast-to-noise ratio between the blood vessel and the background calculated on the clutter filtered power Doppler image according to Equation 1. **b.** Contrast ratio between the blood vessel and the background calculated on the clutter filtered power Doppler image according to Equation 2. **c.** SNR calculated on the enveloped data before clutter filtering according to Equation 3.

3.2 Phantom and *in vivo* B-Mode Results

Qualitative SNR gains in a CIRS phantom and a representative human subject are shown in Figure 4. The SNR gains (dB) using 5 bit, 13 bit, and 5x5 bit codes were 6.42 ± 0.06 , 10.09 ± 0.32 , and 11.32 ± 0.56 in the phantom (N=2) and 2.96 ± 0.43 , 3.03 ± 0.65 , and 3.14 ± 0.51 in transcranial imaging (N=34). The NCC approach underestimated SNR gain *in vivo* due to a low PRF and unmitigated out-of-plane motion, so the amplitudes in bright ROIs were compared, resulting in gains of 4.60 ± 1.33 , 11.55 ± 3.87 and 12.64 ± 2.23 dB. The phantom and *in vivo* results agree with expected gains of 7, 11, and 14 dB.

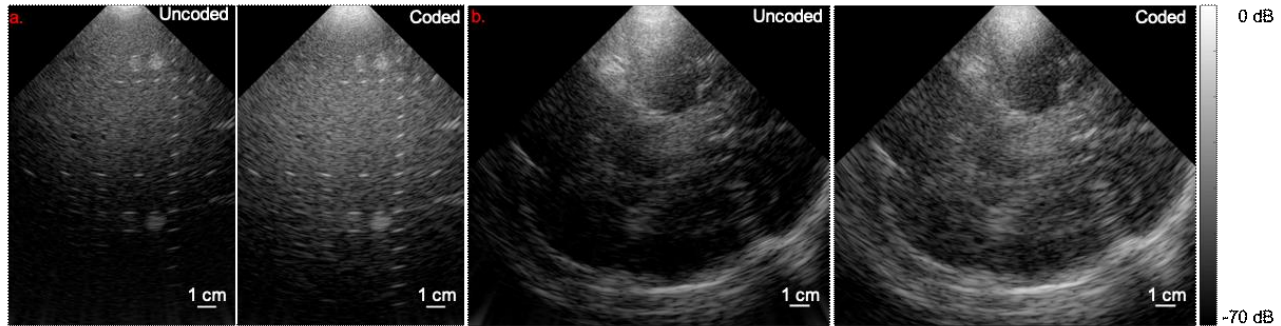


Figure 4: Qualitative comparison of uncoded and 5x5 compound Barker coded excitation approaches. **a.** CIRS phantom. **b.** Transcranial imaging at the temporal window (transverse plane) in a healthy adult male subject. All images shown on same dynamic range.

Transthoracic cardiac B-Mode images are shown in Figure 5, where the coded approach is a 25 bit compound Barker code. Similar to the transcranial images, the NCC approach underestimated SNR gain due to a large amount of unmitigated out-of-plane motion, so amplitudes within the myocardial wall were compared instead, resulting in a gain of 12.04 dB. This result is comparable to the transcranial results and is in line with theoretical expectations.

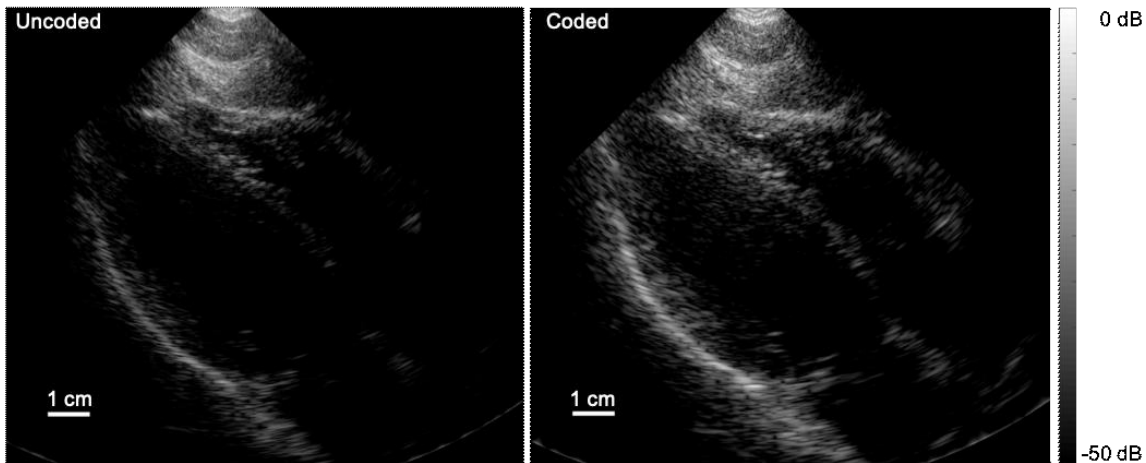


Figure 5: Qualitative comparison of uncoded and 5x5 compound Barker coded excitation approaches in transthoracic cardiac imaging of a healthy adult male subject. Images shown on same dynamic range.

3.3 *In vivo* Blood Flow Results

Finally, to achieve the goal of this work and demonstrate the utility of coded excitation for *in vivo* power Doppler imaging, *in vivo* liver results are shown in Figure 6. The focused B-Mode images along with power Doppler images generated from 50 and 100 frames are shown. The CNR and contrast ratio statistics calculated from the ROIs indicated in Figure 6 are shown in Table 1. From these results it can be seen that, while both uncoded and coded excitation acquisitions benefited from using more frames in the power Doppler image formation, the coded excitation acquisition was able to produce a larger benefit in both CNR and CR in the 50 frame scenario where SNR and blood flow sensitivity are lower. Although

this shallow imaging environment is not particularly challenging, in deeper imaging through more difficult-to-image patients, the benefits of coded excitation would be even more apparent.

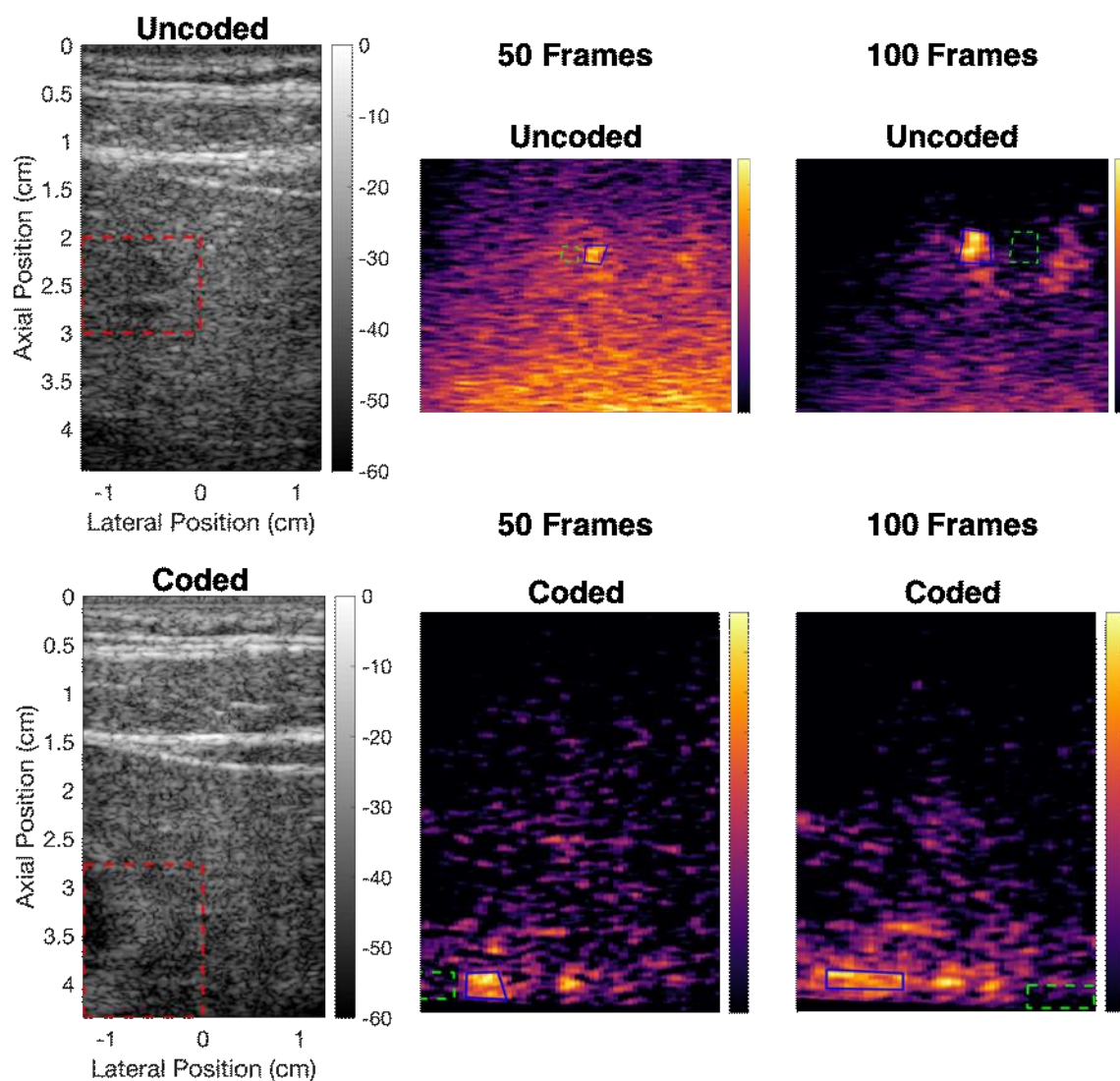


Figure 6: *In vivo* liver imaging results in a healthy adult subject. Gray scale images depict the focused B-Mode images used for targeting. The red dashed boxes indicate the region of the PWSA data that was processed to form power Doppler images, shown in color. In the power Doppler images, green dashed boxes indicate background ROIs and blue solid boxes indicate blood vessel ROIs used for calculating CNR and contrast according to Equations 1 and 2. Power Doppler color bar range is 10 dB in all cases.

Table 1: Comparison of CR and CNR values for *in vivo* blood flow imaging

Frames	Uncoded		Coded		Gain	
	CR	CNR	CR	CNR	CR Gain	CNR Gain
50	2.607 dB	1.840	5.180 dB	2.547	2.574 dB	0.707
100	4.460 dB	2.692	5.128 dB	3.396	0.668 dB	0.704

4. CONCLUSIONS

We demonstrated a novel coded excitation framework for improving the SNR of ultrasound power Doppler imaging that can realize large SNR benefits without compromising axial resolution, contrast, or hardware complexity, unlike previous approaches. We used Field II simulations to predict the benefits that could be realized for power Doppler imaging, highlighting that 1) this approach is able to reliably increase SNR up to theoretical expectations, and 2) coded excitation provides more benefit to CNR and CR in high noise environments. We showed feasibility of *in vivo* application of the coded excitation framework with transcranial and transthoracic B-Mode imaging and demonstrated SNR gains that approach theoretical expectations. Finally, we demonstrated preliminary results of increased CR, CNR, and sensitivity to blood flow due to coded excitation in *in vivo* power Doppler imaging of transabdominal liver imaging. Collectively, the results presented herein suggest that a coded excitation framework consisting of compound Barker codes with inverse filtering pulse compression is a promising platform for increasing the SNR and sensitivity to blood flow signal in challenging *in vivo* imaging scenarios.

ACKNOWLEDGEMENTS

The authors would like to acknowledge the staff at Vanderbilt University's Advanced Computing Center for Research and Education (ACCRES) for their continued support. This work has been supported by the awards T32EB021937 and R01EB020040 from the National Institutes of Health, the award IIS-1750994 from the National Science Foundation, and the National Science Foundation Graduate Research Fellowship Program under grant number 1937963.

REFERENCES

- [1] T. Misaridis and J. A. Jensen, "Use of modulated excitation signals in medical ultrasound. Part I: Basic Concepts and Expected Benefits," *IEEE Trans. Ultrason. Ferroelectr. Freq. Control*, vol. 52, no. 2, pp. 177–191, 2005.
- [2] H. Zhao, L. Y. L. Mo, and S. Gao, "Barker-coded ultrasound color flow imaging: Theoretical and practical design considerations," *IEEE Trans. Ultrason. Ferroelectr. Freq. Control*, vol. 54, no. 2, pp. 319–330, 2007.
- [3] J. Udesen, F. Gran, K. L. Hansen, J. A. Jensen, C. Thomsen, and M. B. Nielsen, "High frame-rate blood vector velocity imaging using plane waves: Simulations and preliminary experiments," *IEEE Trans. Ultrason. Ferroelectr. Freq. Control*, vol. 55, no. 8, pp. 1729–1743, 2008.
- [4] F. Gran, J. Udesen, M. B. Nielsen, and J. A. Jensen, "Coded ultrasound for blood flow estimation using subband processing," *IEEE Trans. Ultrason. Ferroelectr. Freq. Control*, vol. 55, no. 10, pp. 2211–2220, 2008.
- [5] Y. Wang, K. Metzger, D. N. Stephens, G. Williams, S. Brownlie, and M. O'Donnell, "Coded Excitation with Spectrum Inversion (CEXSI) for Ultrasound Array Imaging," *IEEE Trans. Ultrason. Ferroelectr. Freq. Control*, vol. 50, no. 7, pp. 805–823, 2003.
- [6] B. Kiranmai and P. Rajesh Kumar, "Performance Evaluation of Compound Barker Codes using Cascaded Mismatched Filter Technique," *Int. J. Comput. Appl.*, vol. 121, no. 19, pp. 31–34, 2015.
- [7] J. Arendt Jensen, "A model for the propagation and scattering of ultrasound in tissue," *J. Acoust. Soc. Am.*, vol. 89, no. 1, pp. 182–190, 1991.
- [8] J. A. Jensen and N. B. Svendsen, "Calculation of pressure fields from arbitrarily shaped, apodized, and excited ultrasound transducers," *IEEE Trans. Ultrason. Ferroelectr. Freq. Control*, vol. 39, no. 2, pp. 262–267, 1992.
- [9] J. Baranger, B. Arnal, F. Perren, O. Baud, M. Tanter, and C. Demene, "Adaptive Spatiotemporal SVD Clutter Filtering for Ultrafast Doppler Imaging Using Similarity of Spatial Singular Vectors," *IEEE Trans. Med. Imaging*, vol. 37, no. 7, pp. 1574–1586, 2018.